Correlated Neutron-Proton Pairs from the High-Energy Photodisintegration of Helium and Lithium†*

M. Q. BARTON‡ AND J. H. SMITH
University of Illinois, Urbana, Illinois

(Received February 14, 1958)

Observations are made on the protons and neutrons simultaneously ejected from helium and lithium by 280 Mev bremsstrahlung. All photoprotons are found to be accompanied by a neutron. The results are interpreted in terms of Levinger's quasideuteron theory of photodisintegration. The results lead to a measurement of the low momentum spectrum in helium and lithium as well as identification of the high-momentum components of the momentum spectrum as due to two-particle interactions.

I. INTRODUCTION

LEVINGER[1] was the first to propose that the photodisintegration of complex nuclei by photons more energetic than those in the "giant resonance" region proceeded by the absorption of the photon by a neutron-proton pair which he called a quasideuteron. Many of the qualitative features of the early work[2,3] on photoprotons ejected by photons in the region of 100–300 Mev suggested such a mechanism but quantitative proof was lacking. If the photon were absorbed by such a pair in a light nucleus, the chance for both nucleons to escape would be quite good and the observation of a proton and neutron ejected from a complex nucleus in coincidence would prove the existence of such a mechanism. Such correlated pairs of nucleons have been observed by a group at the Massachusetts Institute of Technology and by us.[4] The existence of this effect was quite clear but several questions remained.

1. Were *all* high-energy photonucleons ejected by this two nucleon process?
2. Could the simple theory of Levinger using the effective range theory of nuclear forces give a quantitative picture of the high-energy photodisintegration?
3. Could quantitative observations of this process give a measurement of nuclear momentum distributions?

Questions 2 and 3 have been discussed in two further papers by the M.I.T. group[5,6] and question number 1 has been discussed by Peterson and Roos.[7] This paper will discuss these questions in the light of observations of the photodisintegration of lithium and helium by photons from about 150 to 280 Mev.

II. THEORY

Figure 1(a) shows a schematic diagram for this process. A photon of energy E_γ interacts with a pair of nucleons, a proton and neutron in our case, ejecting them with energies E_p and E_n respectively. The nucleons are each assumed to lose an energy E_{b2} in crossing the boundary of the nucleus (surely a highly suspect approximation for helium and lithium). Furthermore the two nucleons may have an effective binding energy E_{b1} between them in the complex nucleus. The nucleons then emerge into the laboratory with energies $\mathcal{E}_p$ and $\mathcal{E}_n$. We then write

$$E_\gamma = E_p + E_n + E_{b1} = \mathcal{E}_p + \mathcal{E}_n + E_b, \qquad (1)$$

where $E_b = E_{b1} + 2E_{b2}$ is the effective binding energy for the ejection of a neutron-proton pair. E_b includes the excitation of the residual nucleus and the kinetic energy of any other particles which may escape, as well as the actual binding energy of the neutron and proton. It is surely not a constant but will be treated as one here.

The proton and neutron emerge in the laboratory with the proton making an angle θ_p with the photon beam and the neutron an angle θ_n. The plane of the

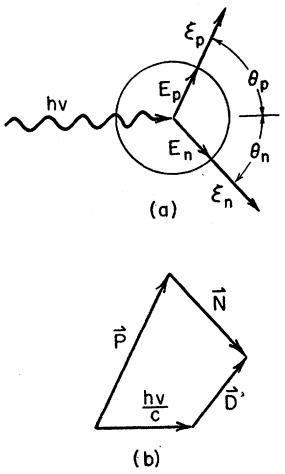

FIG. 1. Schematic diagram for the photodisintegraion of a neutron-proton pair. In (a) the photon of energy $h\nu$ interacts with a pair ejecting the nucleons with energies E_n and E_p. As the nucleons cross the nuclear surface they lose an energy E_{b2} and emerge into the laboratory with energies $\mathcal{E}_n$ and $\mathcal{E}_p$. In (b) is a momentum diagram showing how the various momenta add. **D** and hence **N** have components out of the paper.

† Supported in part by the Office of Naval Research and the U. S. Atomic Energy Commission.

* Parts of this paper are based on a dissertation presented by M. Q. Barton in partial fulfillment of the requirements for the degree of Doctor of Philosophy.

‡ Present address: Brookhaven National Laboratory, Upton, New York.

[1] J. S. Levinger, Phys. Rev. **84**, 43 (1951).
[2] Feld, Godhole, Odian, Scherb, Stein, and Wattenberg, Phys. Rev. **94**, 1000 (1954). See this paper for further references.
[3] J. W. Weil and B. D. McDaniel, Phys. Rev. **92**, 391 (1953).
[4] Myers, Odian, Stein, and Wattenberg, Phys. Rev. **95**, 576 (1954); M. Q. Barton and J. H. Smith, Phys. Rev. **95**, 573 (1954).
[5] Odian, Stein, Wattenberg, Feld, and Weinstein, Phys. Rev. **102**, 837 (1956).
[6] Wattenberg, Odian, Stein, Wilson, and Weinstein, Phys. Rev. **104**, 1710 (1956).
[7] V. Z. Peterson and C. E. Roos, Phys. Rev. **105**, 1620 (1957).

photon and neutron makes an angle ϕ_n with the plane of the proton and photon. This angle is not shown in Fig. 1(a), and all observations have been confined to the plane of the photon and proton, $\phi_n=0$.

A momentum diagram is shown in Fig. 1(b). The outgoing proton and neutron momenta **P** and **N** add to give the sum of the photon momentum E_γ/c and the total momentum of the neutron-proton pair in the complex nucleus, **D**. The momenta **P** and **N** are to be associated with the energies E_p and E_n. In this treatment we assume no refraction at the nuclear surface although this is clearly inconsistent with the assumption of an energy loss. There seems to be no way to differentiate experimentally between such a refraction and the nuclear momentum spectrum.

For a given proton energy and angle and no motion of the neutron-proton pair—the photodisintegration of a real deuteron in the laboratory—the energy and angle of the neutron are completely determined. The existence of a momentum for the pair means that the neutron can come off at a variety of angles centered at the angle for the disintegration of a free deuteron. A measurement of this spread in angle gives a measure of the nuclear momentum distribution.[5]

Following Levinger[1] and Wilson,[8] we note that high-energy photodisintegration by this process involves a large momentum transfer between the two nucleons and hence requires the two nucleons to be close together where the forces are very strong. This is true whether the photodisintegration is in a complex nucleus or in deuterium. Following the spirit of the effective range theory, we then see that the wave function between two nucleons at small distances is determined primarily by their mutual interactions and not by the shape of the wavefunction at large distances. The cross section for disintegrating a neutron-proton pair in a complex nucleus should therefore be proportional to the cross section for the photodisintegration of deuterium, the constant of proportionality being the probability that the two nucleons will be close together in the complex nucleus relative to deuterium. This probability is of course determined by the detailed shape of the wave function for the single nucleon in the complex nucleus. One reservation needs to be made. The neutron and proton in deuterium are primarily in a $^3S_1$ state. In a complex nucleus they can also be in other states. Since the reaction occurs at short range, only S states need to be considered in a rough treatment. However, the $^1S_0$ state can occur. We must therefore write the differential cross section for the photodisintegration of a pair of nucleons in a complex nucleus as

$$\left(\frac{d\sigma}{d\omega}\right)_{np}=\tfrac{3}{4}L_3\frac{NZ}{A}\left(\frac{d\sigma}{d\omega}\right)_{\text{deuterium}}+\tfrac{1}{4}L_1\frac{NZ}{A}\left(\frac{d\sigma}{d\omega}\right)_{\text{singlet}}, \quad (2)$$

[8] R. R. Wilson, Phys. Rev. **104**, 218 (1956).

where Z is the atomic number, N the neutron number, and A the atomic weight. The factors $\frac{3}{4}$ and $\frac{1}{4}$ represent the relative statistical weights of the triplet and singlet states. The constant of proportionality has been written $L(NZ/A)$ following Levinger, since one might expect the probability of a proton and neutron getting close together to be proportional to the number of such pairs (NZ) and inversely proportional to the volume of the nucleus which is proportional to A.

The high-energy cross section for the photodisintegration of deuterium is known quite well experimentally.[9] However, the cross section for a proton and a neutron in a singlet state cannot be determined directly. At lower energies one might trust theoretical calculations. At energies of 150 to 280 Mev mesonic effects are predominant. The triplet state disintegrates both by S-wave and $\frac{3}{2}$, $\frac{3}{2}$ isobaric state transitions.[8] The singlet state can disintegrate only by the S-wave contribution but might be expected to do so with a cross section similar in magnitude to that of the triplet state. The angular distribution of the disintegration of neutron-proton pairs relative to that of deuterium might be expected to throw some light on the subject. Odian[5] showed that the angular distributions were similar showing that L_1 is smaller than L_3 or that the singlet and triplet disintegrations do not have very different angular distributions. For want of a very much better thing to do, we shall assume

$$\left(\frac{d\sigma}{d\omega}\right)_{\text{deuterium}}=\left(\frac{d\sigma}{d\omega}\right)_{\text{singlet}},$$

and write

$$\left(\frac{d\sigma}{d\omega}\right)_{np}=L\frac{NZ}{A}\left(\frac{d\sigma}{d\omega}\right)_{\text{deuterium}}.$$

Any subsequent interpretations of L in terms of the relative probability of two nucleons being near each other in a complex nucleus will be subject to this considerable uncertainty of perhaps 25%.

The probability for producing a photodisintegration of a neutron-proton pair in a complex nucleus by a photon between E_γ and $E_\gamma+dE_\gamma$, with the proton going into $d\omega^*$ in the center-of-mass system, is then

$$d^3\sigma=L\frac{NZ}{A}\left(\frac{d\sigma}{d\omega^*}\right)_{\text{deut}}B(E_\gamma)dE_\gamma d\omega^*, \quad (3)$$

where $B(E_\gamma)$ is the probability that there will be a photon between E_γ and $E_\gamma+dE_\gamma$ in the bremsstrahlung beam, i.e., the bremsstrahlung spectrum. The probability that the particular neutron-proton pair was moving with a momentum between **D** and **D**+d**D** is the square of the momentum wave function for the center of

[9] D. R. Dixon and K. C. Bandtel, Phys. Rev. **104**, 1730 (1956); J. Keck and A. Tollestrup, Phys. Rev. **101**, 360 (1956); Whalin, Schriever, and Hanson, Phys. Rev. **101**, 377 (1956).

mass of the two particles designated $\mathcal{P}(\mathbf{D})$. Thus

$$d^6\sigma = L\frac{NZ}{A}\left(\frac{d\sigma}{d\omega^*}\right)_{\text{deut}}(1-\beta_D)B(E_\gamma)\mathcal{P}(\mathbf{D})dE_\gamma d\omega^* d\mathbf{D}. \quad (4)$$

The factor $(1-\beta_D)$ refers to the change in photon flux due to the motion of the neutron-proton pair, where β_D is the velocity of the center of mass of this pair in units of c. Actually a complete experiment would observe the energy and angle of the proton and neutron in the laboratory, giving

$$d^6\sigma = L\frac{NZ}{A}\left(\frac{d\sigma}{d\omega^*}\right)_{\text{deut}}(1-\beta_D)B(E_\gamma) \times\mathcal{P}(\mathbf{D})J\left(\frac{E_\gamma\omega^* D}{E_n E_p\omega_n\omega_p}\right)dE_n d\omega_n dE_p d\omega_p, \quad (5)$$

where J is the appropriate Jacobian. Our neutron counter did not measure the energy of the neutron, but rather counted all neutrons indiscriminately with an efficiency $\epsilon(\mathcal{E}_n)$. The counting rates are then related to an integral over neutron energies,

$$I_{np} = \frac{d^5\sigma}{d\omega_n dE_p d\omega_p} = L\frac{NZ}{A}\int\epsilon(\mathcal{E}_n)\left(\frac{d\sigma}{d\omega^*}\right)_{\text{deut}}(1-\beta_D) \times B(E_\gamma)\mathcal{P}(\mathbf{D})JdE_n, \quad (6)$$

which, when J is written out, becomes

$$I_{np} = 4L\frac{ZN}{A}Mc^2\left(1+\frac{P^2}{M^2c^2}\right)^{\frac{1}{2}}P\int_{N=0}^{N_{\max}}\frac{B}{EP^*} \times\left(\frac{d\sigma}{d\omega^*}\right)_{\text{deut}}\mathcal{P}(\mathbf{D})N^2dN, \quad (7)$$

where $\mathbf{P}$ is the proton momentum, P^* the proton momentum in the center-of-mass system, E the total energy (practically $2Mc^2$), and the neutron momentum, N, rather than the energy has been used for the variable of integration. M is the rest mass of a nucleon. The counting rate of protons observed regardless of whether they were in coincidence with neutrons, i.e., with the neutron counter turned off, would be related to an integral over both neutron energies and angles without the efficiency factor $\epsilon(\mathcal{E}_n)$.

$$I_p = \frac{d^4\sigma}{dE_p d\omega_p} = 4L\frac{NZ}{A}Mc^2\left(1+\frac{P^2}{M^2c^2}\right)^{\frac{1}{2}}P\int\int\frac{B}{EP^*} \times\left(\frac{d\sigma}{d\omega}\right)_{\text{deut}}\mathcal{P}(\mathbf{D})N^2dNd\omega_n. \quad (8)$$

These two integrals were calculated numerically in the University of Illinois Digital Computer, Illiac, and the numerical integrations are estimated to be accurate to about 1%.

In the calculations, the Schiff[10] zero-degree bremsstrahlung spectrum was used for $B(E_\gamma)$. A polynomial expansion in E_γ and $\cos\theta^*$ which fits all the points given by Keck and Tollestrup[9] within experimental error was used for $(d\sigma/d\omega^*)_{\text{deut}}$. The efficiency $\epsilon(\mathcal{E}_n)$ was a function determined experimentally as described in Sec. III. All necessary dynamics in the transformations and in J were done relativistically, though some completely negligible approximations were made.

For the nuclear momentum distribution a Gaussian,

$$P(\mathbf{D}) = (4\pi ME_0)^{-\frac{3}{2}}\exp(-D^2/4ME_0),$$

was used, where M is the mass of a single nucleon. The comparison between the theoretical results calculated with these integrals and the experimental results will be made in Sec. V.

III. EXPERIMENTAL APPARATUS

This experiment requires the coincident detection of a neutron and a proton, each of energy 50–150 Mev. One expects the two to be correlated such that the counting problem is not appreciably different from that of detecting both particles in the photodisintegration of deuterium.

A. The Proton Counter

Figure 2 shows the arrangement of scintillators used in the proton counter for the first lithium experiments. Counters $1P$, $2P$, $3P$, $4P$, $5P$, and $6P$ were liquid scintillators (3 g p-terphenyl and 10 mg di-phenylhexatriene per liter of phenocyclohexane) in Lucite cells. For later experiments, including the helium data, $1P$, $2P$, and $3P$ were replaced by thinner counters of Fullman plastic. Counters $1C$ and $2C$ were plastic

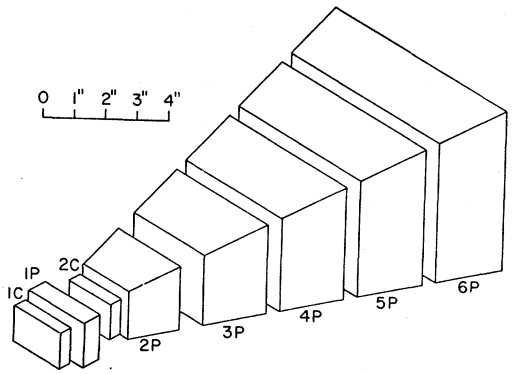

FIG. 2. An isometric drawing of the active scintillator volumes used in the first experiment on lithium. C scintillators are used to trigger the apparatus. Pulse heights are measured in P scintillators. For the helium experiments the liquid scintillators $1P$, $2P$, and $3P$ were replaced by thinner plastics.

[10] L. I. Schiff, Phys. Rev. 83, 252 (1951).

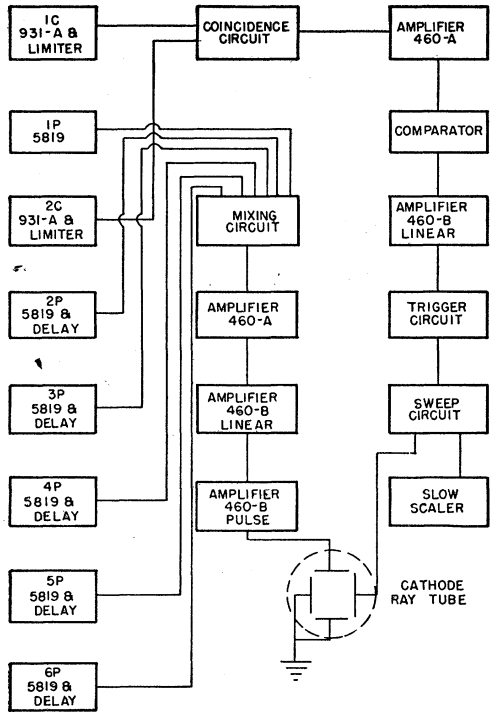

FIG. 3. Block diagram of the electronics. The coincidence circuit used had a resolving time of about 6 millimicroseconds.

scintillators (Scintillon, Pilot Chemical Company). $2C$, the counter which determined the solid angle of the proton counter was 3.01 cm high by 3.97 cm wide and was placed 39.52 cm from the target center. As is shown in the block diagram of the electronic apparatus in Fig. 3, the output of $1C$ and $2C$ were mixed in a Rossi-type diode coincidence circuit whose output was used to trigger the sweep circuit of an oscilloscope. The outputs of each of the other scintillators were appropriately delayed, integrated for about 40 mμsec, mixed, amplified, and displayed on the vertical plates of the oscilloscope. Thus each charged particle entering the telescope as far as $2C$ resulted in an oscilloscope sweep with one to six pulses, depending on the range of the particle. Each such sweep was photographed and the data were read from the film with a simple projector. Figure 4(a) shows the correlation between the first two pulse heights for events that do not enter $3P$. Because of the difference in their specific ionizations, different charged particles fall on different loci on this chart. Those mesons which make stars in the second counter have larger second pulses than expected on the basis of ionization losses. Figure 4(b) shows a chart of three pulse events. The correlation between the two final pulses is similar to that shown in Fig. 4(a) for two pulse events. Since the counters are somewhat thicker in this case, there is a larger signal at the photomultiplier; consequently the resolution is slightly better. If one neglected the third pulse and plotted these events on Fig. 4(a) along with two pulse events, the protons of Fig. 4(b) would overlap the group classified as meson stars. This confusion, however, is avoided by the presence of the third pulse. The first pulse of each event of Fig. 4(b) (not shown on the chart) is required to be consistent with that of the other events of the group.

Similarly, charts can be drawn for four, five, and six pulse events so that each chart shows the final two pulses along the particle's range. The events can then be classified as in Fig. 4, with the additional requirement that all of the earlier pulses along the particle's range be consistent with the classification. The time position of each pulse on the oscilloscope sweep is also useful in rejecting background events.

Events counted in this manner have the obvious disadvantage of being tedious to analyze. There are many advantages, however, which can hardly be accomplished by purely electronic means. The counter is simple and inexpensive and permits an unambigious identification of most of the events. Although the usual corrections for scattering and mistaken identity still apply, they are minimized in this counter by the large amount of information available for each event. Finally, the data can be sorted into any arbitrary number of energy groups and the data can be collected simultaneously, permitting a most efficient use of betatron time. If the range to each counter is used to define the particle's energy, as was done in this experiment, there are six well distributed groups whose energy is nearly independent of electronic stability.

As can be seen from Fig. 4, occasional events are difficult to classify. For one-pulse events in this experiment, a division between the meson and proton groups was chosen such that the number of protons omitted should be equal to the number of mesons counted by mistake. For two-pulse events, an empirical division line was used. It is believed that the uncertainty in number of protons is less than 3% in both cases. For events with three or more pulses, this uncertainty is even less because of the large amount of information available.

The data must also be corrected for losses due to scattering in the telescope. Because of the large taper in the counter, the correction for multiple Coulomb scattering or for elastic diffraction scattering is negligible. The only sizable scattering correction is for inelastic scattering from carbon and elastic scattering from hydrogen. Clearly the correction for scattering is not completely independent of the criterion for accepting a proton pulse described in the previous paragraph, because a proton scattered early in this range will give rise to a set of pulses which, in general, will be quite different from that of a proton which comes to rest. The scattering corrections which were used for this experiment were calculated by assuming a geometric cross section $\sigma=\pi R^2$ ($R=1.4\times10^{-13}\,A^{\frac{1}{3}}$) for carbon and experimental cross sections for p-p scattering.[11] The cor-

[11] E. Segrè, *Experimental Nuclear Physics* (John Wiley and Sons, Inc., New York, 1953), Vol. I.

rections include estimates of the numbers of protons counted in the wrong range bins because of scattering.

Since the film in the oscillograph record camera cannot be advanced during a yield pulse of the betatron, the sweep circuit of the oscilloscope was made so that two sweeps could not occur during the yield pulse to prevent multiple exposures of the film. This necessitates a correction for counting losses which is small if the intensity of the betatron is so adjusted that the average number of events per pulse is much less than unity. This correction can be obtained very accurately by connecting a fast scaler to the output of the trigger circuit and a slow scaler to the sweep circuit. Thus one has a means of comparing directly the true counting rate with the number of events photographed. This correction was negligible for all coincidence runs and never greater than 5% for runs in which protons only were observed.

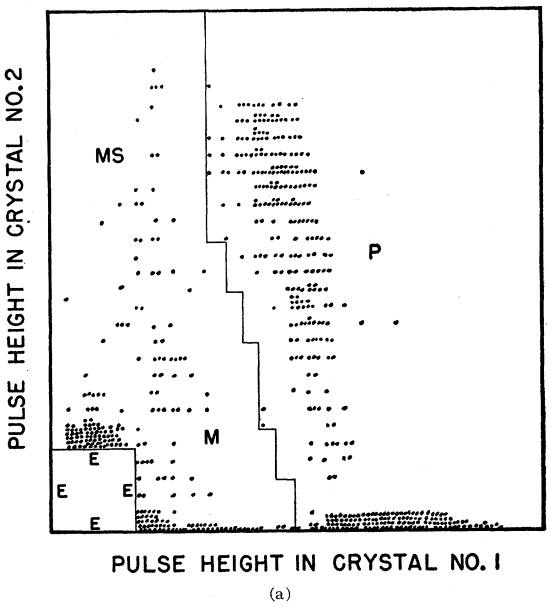

(a)

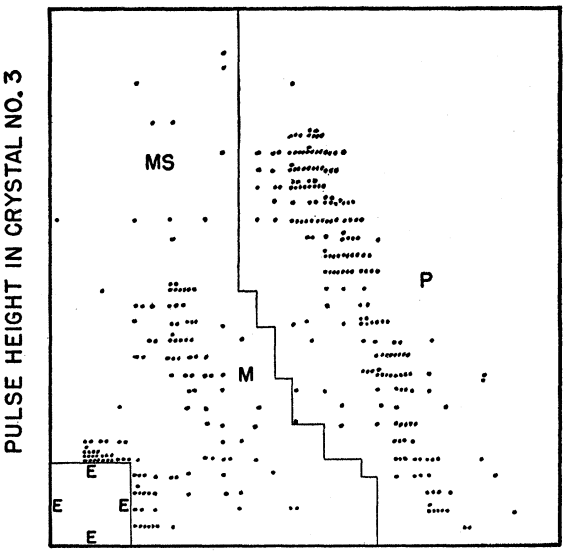

(b)

FIG. 4. Pulse heights for events in the first three scintillators. In (a) are plotted the pulse heights of events which gave pulses only in the first two scintillators. The large group at the bottom are events with pulses in $1P$ only. At (b) are events with pulses in $1P$, $2P$, and $3P$, but not in $4P$. Events marked E are electrons, the region inside the rectangle being very full of pulses. Events marked M are mesons, MS meson stars. P events are protons, the line showing the arbitrary division used in this experiment.

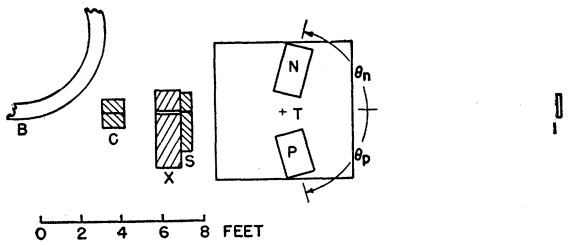

FIG. 5. The layout of the apparatus. B is the betatron; C, the lead collimator; X, a borax neutron shield; N and P, the neutron and proton counters; T, the target; I, the ionization chamber monitor.

B. Neutron Counter

The neutron counter was a glass cylinder ($3\frac{3}{4}$-in. inside diameter by 10 in. long) containing liquid scintillator (3 g p-terphenyl per liter of phenolcyclohexane) viewed by a single 6199 photomultiplier. The front surface of the counter was 32.86 cm from the target center. Neutrons were detected by observing the recoils from the neutrons scattering off of the nuclei of the scintillator itself. Since charged particles or photons cannot penetrate the two-inch lead wall in front of the counter, the large pulses in this counter are attributed to neutrons. The output of the counter was limited and mixed with $1C$ and $2C$ of the proton counter in the coincidence circuit. This circuit could be switched off so that the neutron coincidence was not required. This neutron counter was intended to be used as one channel of a coincidence circuit and would not be useful independently.

C. Experimental Arrangement

The experiment was set up as shown in Fig. 5. Photons from the betatron passed through a lead collimator placed between adjacent back legs of the betatron C magnet, a borax neutron shield, a secondary lead collimator, and impinged on the target placed at T. The intensity of the beam was determined with a flat ion chamber placed at I. For the lithium runs the target was a paraffin coated block of lithium 2 in. long in the beam direction and 1 in. wide. The liquid target[12] used

[12] E. A. Whalin, Jr., and R. A. Reitz, Rev. Sci. Instr. **26**, 59 (1955).

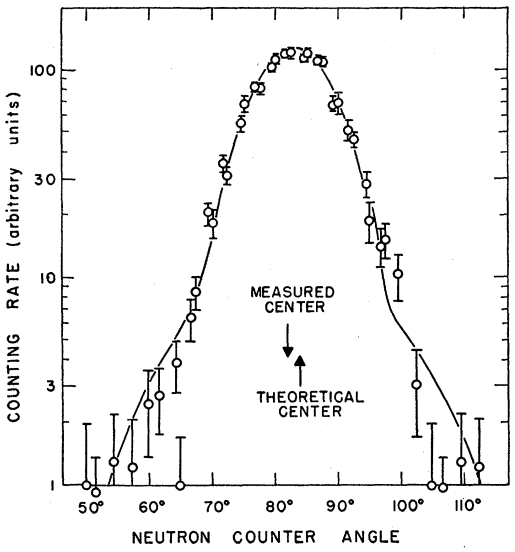

FIG. 6. Deuterium coincidence counting rate *vs* angle of the neutron counter.

for the deuterium and helium data provided a vertical cylinder of liquid 2 in. in diameter. Both targets and the ion chamber were sufficiently large to eclipse the entire collimated beam which was $\frac{11}{16}$ in. at the target position. Figure 7 also shows the counters in typical positions. Both counters could be rotated about the target in the horizontal plane but the data described in this paper were all taken with the proton counter at $\theta_p=75°$. The counters were enclosed in 4-in. lead walls except for a 4-in.×4-in. entrance to the proton counter and a 2-in. wall in front of the neutron counter. For most of the experiment the betatron was operated at an energy of 280 Mev with a 200-μsec yield pulse corresponding to an energy spread of 3%. For the earlier lithium data the energy was 285 Mev and the yield pulse was 270 μsec long.

D. Test Procedures

The first series of betatron runs was used to prove that the electronic circuits were operating satisfactorily. By determining the proton counting rate as a function of the voltage on 1*C* and 2*C*, and as a function of the relative delay between 1*C* and 2*C*, it was established that protons were detected with essentially 100% efficiency. Although plateaus were not expected for the neutron counter, tests showed that its efficiency was sufficiently insensitive to electronic parameters to permit stable operation. A complete test of the proton counter was done by observing the photoprotons from the photodisintegration of deuterium. The differential cross sections at 75° in the laboratory for several energies as derived from the test data are summarized in Table I. Within the statistical uncertainty these results can be considered in agreement with the results of Keck and Tollestrup.[9]

The neutrons from the photodisintegration of deuterium also provide a means of testing the neutron counter. Because of the two-body kinematics of this process, there is for each proton energy and angle a unique neutron energy and angle. Thus it was possible to prove that the counter was performing properly and to measure its efficiency. Figure 6 shows the coincidence counting rate as a function of the angular position of the neutron counter. The results of each of the four bins have been independently normalized and shifted by the amount predicted by kinematics to permit superposition on the graph. The angular shift is seen to be in agreement with that predicted by kinematics, except that there is a systematic angular shift which is probably due to a slight displacement of the liquid target. The curve shown through the points is the angular resolution of the target counter geometry as calculated by a Monte Carlo method using the Illiac computer. This calculation included scattering from the lead house. By comparing the normalization of the angular curve for each bin with the proton-only data from the same bin, one obtains the efficiency of the neutron counter for that energy. Figure 7 shows these results. The curve shown is the empirical choice used for $\epsilon(\mathcal{E}_n)$ as described in the previous section.

The lower-energy cutoff shown is an approximation, but a good one, based on the time resolution of the coincidence circuit. For the proton energies used, neutrons slower than about 20 Mev would not be in coincidence. The exact shape of $\epsilon(\mathcal{E}_n)$ at low energies does not affect the theoretical results appreciably.

E. Background

For runs taken with the proton counter in coincidence with the neutron counter, no-target backgrounds were entirely negligible. When protons only were counted, the 2-mil brass walls of the liquid container gave a background in the neighborhood of 7%.

The paraffin coating on the lithium target was treated as if it were lithium. It made up about $\frac{1}{2}$% by weight of the thickness of the target.

TABLE I. Deuterium laboratory cross sections compared to those of Keck and Tollestrup.[a] The points at 146, 187, and first run at 248 Mev were taken during the first betatron run of this experiment. The others during the second. The figures for Keck and Tollestrup are taken from their reconstructed curve. Errors are rms counting statistics.

E_γ (Mev)	$d\sigma/d\omega$ (microbarns/sterad) This experiment	Keck and Tollestrup
129	5.5±0.5	5.3
146	5.0±0.4	5.2
154	5.6±0.4	5.3
187	6.1±0.4	5.6
194	5.6±0.4	5.7
248	6.1±0.4	6.0
248	6.0±0.4	6.0

[a] See reference 9.

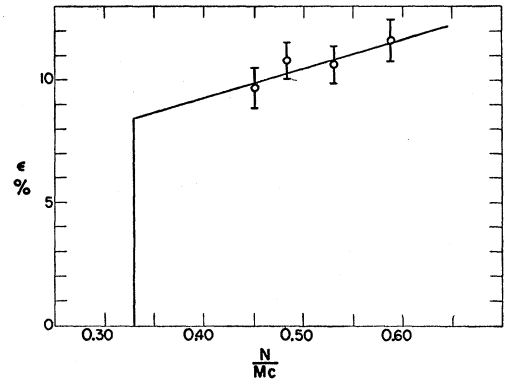

FIG. 7. The peak efficiency of the neutron counter *vs* momentum of the neutron before leaving the nucleus. The curve shown is typical of those used in the numerical calculations. The points are measured points. The curve would be different for each different value chosen for E_{b2}. There is no justification for the straight-line curve other than simplicity in calculation.

Accidental backgrounds were completely negligible when protons only were counted. However, accidental coincidences between a real particle going down the proton telescope and something in the neutron counter were quite troublesome, particularly when the neutron counter was at forward angles. At 40° the accidental background provided 66% of the "neutron"-proton coincidences from lithium. At other angles the situation was much better. At 75°, 6% of the "neutron"-proton coincidences were accidental. For helium the accidentals at 75° were only 2%, and at 40° about 40%. At all angles a large number of accidental coincidences were observed between "neutrons" and electrons and mesons. Once the ratio between these and accidentals between "neutrons" and protons was determined, the number of nonproton accidentals could be used to monitor the proton accidentals.

IV. RESULTS

The principal results of the experiment are shown in Figs. 8 through 13. Figures 8 and 9 show the coincidence counting rate between protons of various energies and neutrons as the neutron counter is swung in angle. The counting rate goes through a maximum at approximately the angle expected for the photodisintegration of deuterium. However, the curves are considerably wider than the counter resolution curve shown in Fig. 6 clearly showing the effect of the nuclear momentum distribution. All these curves were taken with the proton counter at 75° to the photon beam. One other run was taken with the proton counter at 50° to the beam and the maximum of the peak shifted back to the appropriate angle predicted by deuteron dynamics.

It is of additional interest to know the energy distribution of the protons which are ejected in coincidence with the neutrons. As a measure of this, the total number of coincidence counts observed in each proton energy bin are plotted *vs* proton laboratory energy in Figs. 10 and 11. Such a number has no physical significance since different amounts of time were spent counting at different neutron counter angles. However, the numbers so obtained may be compared with a theory

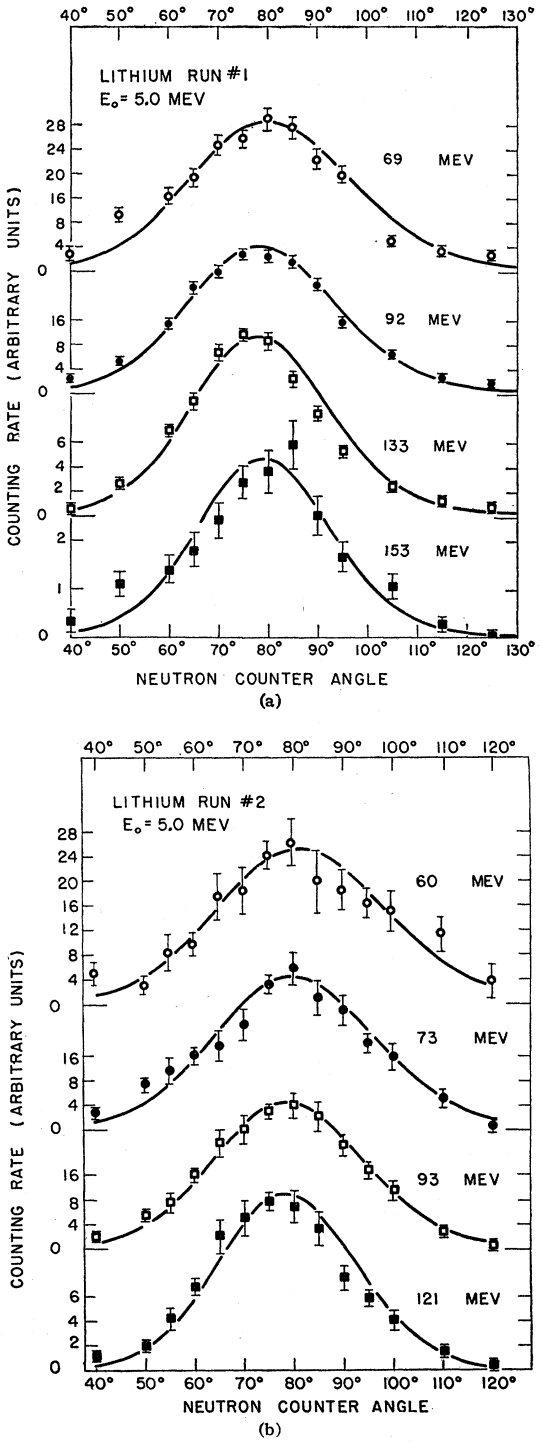

FIG. 8. Lithium coincidence counting rate *vs* angle of the neutron counter.

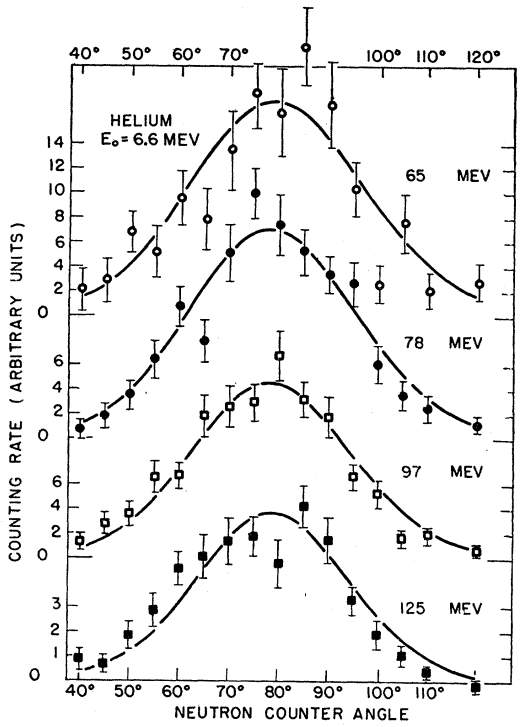

FIG. 9. Helium coincidence counting rate *vs* angle of the neutron counter.

normalized in the same way. It would have been better to have used a large neutron counter like Odian's[4] for this type of measurement. The graphs in Figs. 10 and 11 show clearly the sharp drop in the number of photoprotons coincident with neutrons at proton energies greater than half the bremsstrahlung maximum. The fact that any at all are observed with these large energies is again due to the nuclear momentum distribution, and the rate at which the fall with energy occurs is another measure of the magnitude of these nuclear momenta.

Figures 12 and 13 show the number of photoprotons observed as a function of energy of the photoprotons when the neutron counter was turned off. This is the same type of data as is available from many of the older experiments. Again the drop at one-half the betatron energy is observed.

V. COMPARISON WITH THEORY

The main purpose of this experiment was to see how well a simple two-nucleon interaction could account for the high-energy photodisintegration of complex elements. In the analysis of the data the binding energies E_{b1} and E_{b2}, the internal momentum parameters E_0, and the relative probability L for a neutron and proton to be close together, are all treated as adjustable parameters. How well the values obtained compare with what we know of complex nuclei will determine how successful the simple theory is.

Unfortunately, one more complication must be faced before a detailed comparison between theory and experiment can be made. Even if the primary interaction is between a photon and a two-nucleon system, one or both of these nucleons can suffer a collision with another

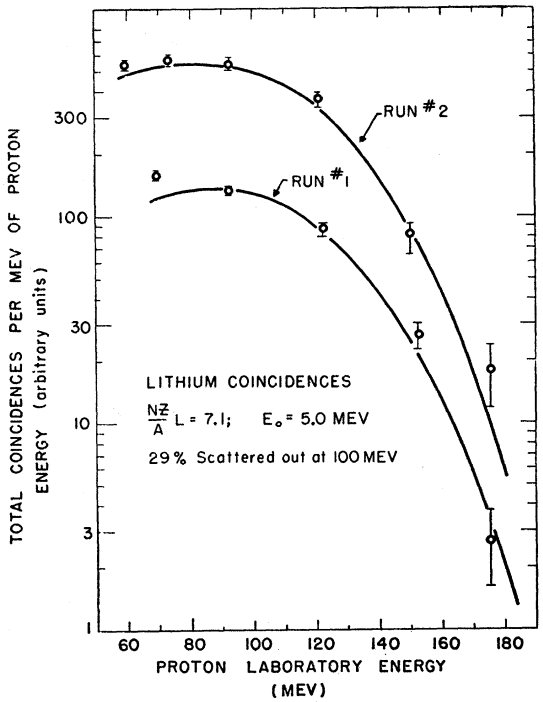

FIG. 10. Total coincident counts per Mev of proton energy from lithium *vs* the proton laboratory energy.

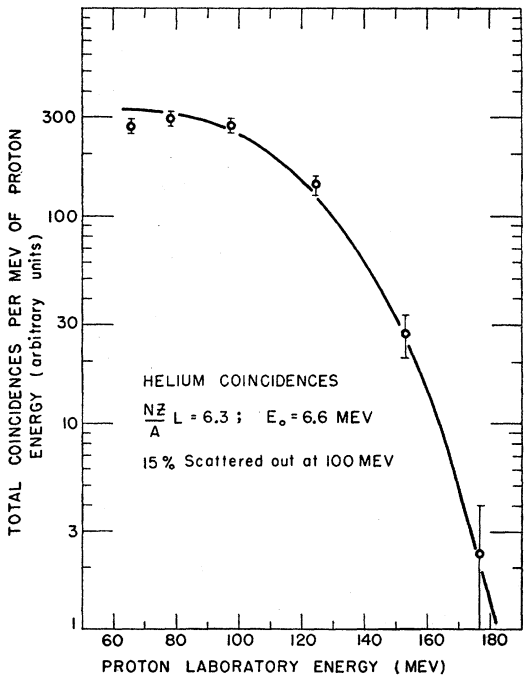

FIG. 11. Total coincident counts per Mev of proton energy from helium *vs* the proton laboratory energy.

nucleon in the same nucleus before leaving. If the probability for a nucleon making such a collision is α, the probability for its escape without scattering is $(1-\alpha)$. We assume, though it is only an approximation, that the probability for both nucleons escaping is $(1-\alpha)^2$. We further assume that the energy dependence of α is just the average of the n-p and p-p scattering cross sections, but we leave the normalization of α to be found experimentally.

The method used to determine the parameters E_{b1}, E_{b2}, E_0, L, and α from the experiment can best be described as guided trial and error. Each affects the other to some extent, but fortunately each is determined primarily by some outstanding feature of the experiment.

A. Determination of E_0

Perhaps the most prominent feature of these experiments is the spread in angle of neutrons in coincidence with protons caused by the internal motion of the nucleons, characterized in our interpretation by the parameter E_0. Referring to Fig. 1, it is easy to see that the angle from the center of the curve to the $1/e$ point should be approximately $(4E_0/E_n)^{\frac{1}{2}}$, where E_n is approximately E_p. A more accurate value for E_0 can be obtained from the numerical integrations described in Part I after account has been taken of the counter resolution. E_0 is thus determined primarily by the curve width. Since E_p and not the laboratory energy enters the expression for the curve width, the value of E_0 depends somewhat on the value chosen for E_{b2}. The other parameters do not affect the choice for E_0 appreciably.

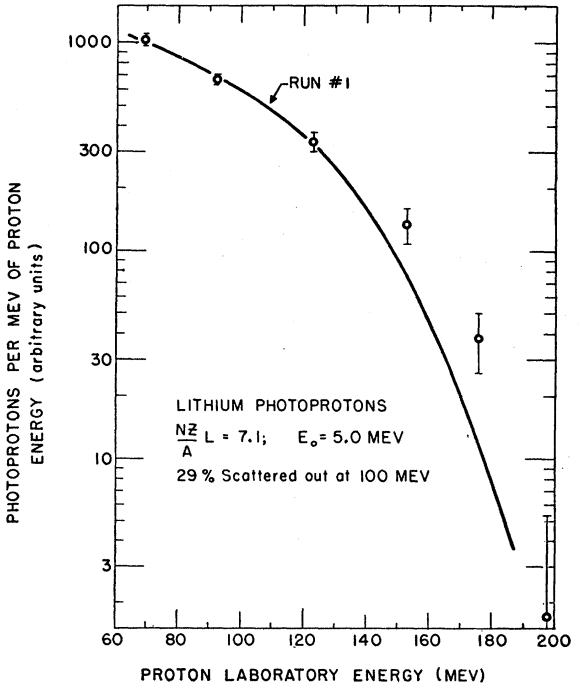

FIG. 12. Total proton counts per Mev of proton energy from lithium *vs* the proton laboratory energy. During the second lithium run, insufficient data were taken to justify a separate curve.

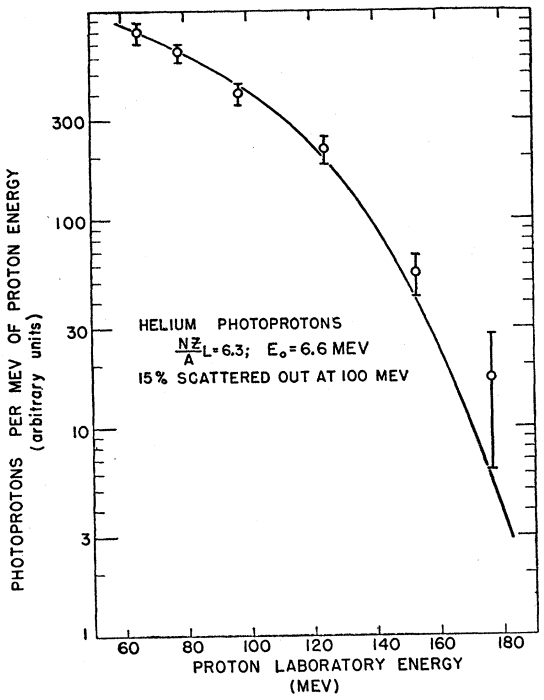

FIG. 13. Total proton counts per Mev of proton energy from helium *vs* the proton laboratory energy.

It should be emphasized at this point that this experiment measures the momentum of the center of mass of a neutron proton pair. This particular information is different from that obtained in most measurements of the momentum of single nucleons and has some interest of itself. However, it would also be interesting to compare this measurement with the momentum of single nucleons. To make this comparison for light nuclei, it is necessary to take account of the fact that the center of mass of the nucleus must remain stationary. If p_i is the momentum of the ith nucleon, then

$$\sum_{i=1}^{A} p_i = 0.$$

Squaring and averaging gives

$$\sum_{i=1}^{A} \langle p_i^2 \rangle + \sum_{i,j} \langle p_i p_j \rangle = 0.$$

If we then assume that $\langle p_i^2 \rangle$ is the same for all the nucleons and $\langle p_i p_j \rangle$ is the same for all pairs, then

$$A\langle p_i^2 \rangle + A(A-1)\langle p_i p_j \rangle = 0. \tag{9}$$

The mean square of the sum of two momenta is

$$\langle (p_1+p_2)^2 \rangle = 2\langle P_1^2 \rangle + 2\langle p_1 p_2 \rangle. \tag{10}$$

From (9) and (10), we obtain

$$\langle(p_1+p_2)^2\rangle=2\left(\frac{A-2}{A-1}\right)\langle p^2\rangle. \quad (11)$$

The well-known relation from kinetic theory gives, for a Gaussian distribution, the average energy of the center of mass as $\frac{3}{2}E_0$, and Eq. (11) then gives

(average energy of a single nucleon)

$$=\tfrac{3}{2}\left(\frac{A-1}{A-2}\right)E_0. \quad (12)$$

The approximations made in this derivation are probably fairly good for helium. However, in heavier nuclei the relations can be considered only roughly correct.

B. Determination of E_{b1} and E_{b2}

The total effective binding energy $E_b=E_{b1}+2E_{b2}$ is very quickly determined from the curves of Figs. 10 and 11. A total binding energy is guessed, and theoretical values for the total number of coincidences observed at various proton energies are determined. In general, if the total binding energy is incorrect, the break in the curve will occur at the wrong proton energy. An adjustment is easily made. The error in the total binding energy can be inferred by noting how far the curves in Figs. 10 and 11 can be slid horizontally and still made to fit the experimental points.

At first the total binding energy was ascribed to E_{b1}, the binding between the two nucleons. This was clearly incorrect, for the neutrons in coincidence with protons would go too far forward. Next the total binding energy was ascribed to E_{b2}. The curves were still slightly too far forward. The fit became somewhat better when both E_{b1} and E_{b2} were admitted, with E_{b1} being negative, i.e., by ascribing a positive total energy to the two-nucleon system. A positive energy would be expected because of the internal momentum distribution.

Actually only the sum $E_b=E_{b1}+2E_{b2}'$ is determined with any accuracy. $E_{b1}=0$ would fit the data only slightly less well than the $E_{b1}=-10$ Mev actually used. Splitting the binding energies in this way is surely a naive concept. The misfit in angle of the higher energy bins in Figs. 8 and 9 may be due to the very simplified picture used for the binding energies.

TABLE II. Summary of the constants used to construct the theoretical curves of Figs. 8 to 13. The errors are based on our judgment of possible limits for the parameters and are never limited by statistics. E_{b1} is only a rough guess.

	$L(NZ/A)$	E_0 Mev	E_b Mev	E_{b1} Mev	E_{b2} Mev	α at 100-Mev nucleon energy
Helium	6.3 ±1.0	6.6±1.2	45±5	−10	27.5	0.15±0.05
Lithium	7.05±1.0	5.0±1.0	25±5	−10	17.5	0.28±0.05

C. Determination of α

The fraction of the nucleons which are scattered in leaving the nucleus is very easily determined in principle. The total number of protons which are in coincidence with neutrons is determined by integrating under the curves of Figs. 8 and 9, using the theoretical expressions for the shapes out of the plane and taking account of the neutron-counter efficiencies. This integration will give $(1-\alpha)^2$ times the number of primary events, since a scattering of either particle, being nearly isotropic at these energies, will essentially remove the event from the counting region. On the other hand, counting the protons only will give $(1-\alpha)$ times the number of primary events, since a scattering of the neutron is inconsequential. The ratio of these numbers, then, gives $(1-\alpha)$.

An accurate determination of $(1-\alpha)$ depends proportionately on an accurate knowledge of the neutron counter efficiency. This was measured to about 5%. Furthermore, the method assumed that there is no other source for photoprotons except such two particle reactions. If α turns out to be abnormally high, it might mean that there were some other such source of protons.

Actually, in comparing coincidence to single proton counting rates, another correction must be made. A proton observed at one energy may have been created at a greater energy and scattered into the lower-energy bin. This correction was made by the method of Weil and McDaniels.[3] It amounted to about a 50% correction to α.

In this way α's were computed for each energy bin and were found to be consistent with the assumption that α varied with energy like the average of the n-p and p-p cross sections. The best experimental fit to this assumption was made and the theoretical curves were corrected for this scattering in the nucleus.

D. Determination of $L(NZ/A)$

After all the other parameters are found, $L(NZ/A)$ is determined by the normalization which best fits all the data.

E. Best Fits to Parameter

Table II lists the parameters obtained by the trial-and-error fitting process described in this section. The curves of Figs. 8 through 13 were computed using these parameters. The angular correlation curves of Figs. 8 and 9 were individually normalized. However, the amount of normalization required can be estimated from Figs. 10 and 11.

It is very difficult to estimate an error for the various numbers given in Table II. The errors quoted are our guesses, not intended to be conservative. We should be surprised if the actual errors were twice those quoted.

VI. DISCUSSION

Comparison of the experimental results to the calculated curves in Figs. 8 through 13 shows that it is quite possible to construct a theory based on two-nucleon interactions which will satisfactorily explain the major aspects of high-energy photodisintegration and do so with detailed agreement with experiment. It remains only to compare the numbers found from the empirical curve fitting with what we know about nuclear structure.

A. Helium

The curves based on a Gaussian momentum spectrum fit the data for helium quite well. Whether this indicates a basic single-particle Gaussian momentum spectrum or whether it represents the central limit theorem at work after the folding of two single-particle spectra and a resolution curve is not clear. At any rate, the actual momentum spectrum cannot be far different from a Gaussian. Application of Eq. (12) to the value $E_0=6.6$ Mev found for helium gives an average kinetic energy of 14.8 Mev for a single particle.

In the case of helium, we may make a somewhat more detailed comparison to Hofstadter's measurements on the root-mean-square radius of helium. Using Irving's wave function,[13]

$$\psi \propto \exp[-\alpha(\tfrac{1}{2}\sum_{i,j=1}^{4}(r_i-r_j)^2)^{\frac{1}{2}}],$$

a relation can be found between the root-mean-square radius and the average value of the sum of the momenta of two particles. This gives

$$\langle r^2\rangle=\frac{45}{32\alpha^2};\quad \langle(p_1+p_2)^2\rangle=\tfrac{4}{3}\hbar^2\alpha^2,$$

and finally

$$\langle r^2\rangle=\frac{15}{8}\frac{\hbar^2}{\langle(p_1+p_1)^2\rangle}=\frac{5}{16}\frac{\hbar^2}{ME_0}.$$

Upon using our value of E_0, this gives

$$r_{\rm rms}=(1.40\pm0.12)\times10^{-13}\text{ cm}.$$

Hofstadter[14] gives a value of 1.61×10^{-13} cm, which becomes 1.41×10^{-13} cm upon taking account of the charge distribution in the proton while considering that of the neutron negligible. The agreement with this latter value is striking, but it is not completely clear that the larger value should be excluded.

It should be emphasized here that the spread in angle of the neutron correlation gives a measure of the low-momentum components which should be calculable with a wave function like Irving's. The existence of the two-body high-energy photoeffect shows that high-momentum components are present in the wave function and that they should be associated with two-particle interactions.

The effective binding energy of 45 Mev for helium can be qualitatively understood as the sum of the actual binding energy (28 Mev) and the kinetic energy of the recoiling nucleons. If we assume that the two remaining nucleons maintain the kinetic energy they had before the event (the "sudden" approximation), we would predict a binding energy of $28+2\times14.8=57.6$ Mev. Actually the data are weighted somewhat so as to favor events in which the center of mass of the remaining nucleons is not moving. This gives an expected value of $E_b=54$ Mev. Interactions in the final state will reduce this figure still further, so that a value of $E_b=45\pm5$ Mev is quite reasonable.

The value of $E_{b1}=-10$ Mev should be considered only as an indication that the two particles of the neutron-proton pair have relative kinetic energy when they are far apart. As a matter of fact, a value $E_{b1}=-19$ Mev might be more nearly what one expects. Such a value would be consistent with the experiments.

The value for $\alpha=0.15$, the fraction of 100-Mev particles strongly scattered after the primary interaction, is quite reasonable when compared to the expected mean free path through nuclear matter. Looked at from another point of view, we might say that 15% of the time each of the particles in the pair is also strongly interacting with a third particle.

The fact that α is small and is a reasonable value suggests that there are no other important mechanisms for the production of high-energy protons except interaction of photons with n-p pairs. Any such mechanism would give protons without neutrons and lead to a high value for α.

At the highest energies shown in Fig. 13 it is seen that there are more protons than predicted by the theory. One possibility is that these are protons from the $He^4(\gamma,p)He^3$ reaction. They are to be associated with γ rays of about $\frac{4}{3}E_p$ rather than about $2E_p$ as with the protons from neutron-proton pairs. They therefore are a small part of the total photodisintegration cross section. We estimate about 3.5%.

The total cross section for the process shows that photodisintegration of a helium nucleus is 6.3 times as probable as the photodisintegration of a deuteron. Levinger calculated 6.4 NZ/A for a heavy nucleus. The "agreement" with our result has little significance other than to show that our result is reasonable. Using the somewhat naive assumption that the probability for photodisintegrating a neutron-proton pair in helium is proportional to the probability that they are within 1.4×10^{-13} cm of each other compared to the probability that they are within 1.4×10^{-13} cm of each other in deuterium, one finds that photodisintegration should be 5.2 times as probable in helium as in deuterium when one uses the Irving wave function for helium (with α chosen to agree with our momentum measurements and hence with Hofstadter's measurements) and the Hulthén

[13] J. Irving, Phil. Mag. **42**, 338 (1951).
[14] R. Hofstadter, Revs. Modern Phys. **28**, 214 (1956).

wave function for deuterium. This can be considered to be satisfactory agreement with our experiment.

B. Lithium

The value of the binding energy $E_b=25$ Mev indicates than an α particle must be left bound a substantial fraction of the time. An energy of 11 Mev is necessary to remove the neutron-proton pair and leave He^4+n. Some kinetic energy would also be left in these fragments. It is clear that the additional energy of 20 Mev necessary to break up the α particle is provided in only a fraction of the disintegrations. Since the observed total cross section requires that the central core of the lithium be broken up most of the time, it means that the probability for the nuclear fragments to rearrange themselves into an α particle must be quite high.

The fraction of each of the particles scattered after the primary interaction is 28% at 100 Mev. This value is quite reasonable on any grounds and, if extrapolated to a nucleus the size of carbon, would indicate that about 35% of each type of particle should be scattered. When one takes into account the uncertainties, this can be considered to be satisfactory agreement with the 45% found by Weil and McDaniel[3] for carbon.

For lithium, no direct comparison can be made between the momentum spectrum observed and radius measurements. However, we can compare our results directly to the M.I.T. results[6] for lithium. Our value of 5.0 ± 1.0 Mev compares very badly with their value of $E_0=9\pm1$ Mev. The data are treated very differently in the two experiments, theirs with a more convenient and effective approximation, ours with a more cumbersome but presumably more accurate numerical integration. In the region where they should agree, the two theoretical methods give identical results except for a small angular shift. The cause for part of the discrepancy may be in differences in treatment of the counter resolution problem, but this can be only part of the trouble. Further experiments will be needed to find the discrepancy.

A glance at the curves in Fig. 8 show that we find no direct evidence for two distinct momentum distributions as proposed by Wilcox and Moyer.[15] However, this could have been obscured by our counter resolution. In fact, it is possible to treat our lithium results by assuming that there is an α-particle core which behaves like a free α particle and a diffuse cloud around it containing two neutrons and a proton with effectively zero internal momenta.

The total cross section observed is 7.05 times that from deuterium. Of this, 6.3 is supposed to be contributed by the core, leaving 0.75 to be contributed by the outer nucleons by themselves (2 pairs) and interacting with the core (6 pairs). The core is supposed to have $E_0=6.6$ Mev, the cloud pairs $E_0=0$ Mev, and the interaction pairs $E_0=6.6/2$ Mev. The resulting addition gives a curve looking exactly like the one observed which would be characterized by a single E_0 of 5.0 Mev. The low probability for interaction with cloud nucleons would mean a very diffuse cloud, characterized by a root-mean-square radius of perhaps 3.7×10^{-13} cm. This would give a total root-mean-square radius for lithium of about 2.4×10^{-13} cm. Despite the excellent agreement with the Stanford measurements,[14,16] it seems to be somewhat over-optimistic to believe in this treatment in detail. It does remain a possibility, however.

Figure 12 again shows too many high-energy protons. Again the explanation may be that these are protons recoiling against heavier portions of the nucleus. The percentage of these events at the appropriate photon energy is again small.

VII. CONCLUSIONS

There seems to be little doubt that nearly all high-energy photodisintegrations leading to the emission of a high-energy proton proceed by the interaction of a photon with a neutron-proton pair. Since these are interactions in which the nucleons leave the nucleus with large momenta, we may conclude that the high-momentum components of the nuclear wave function come from such two-particle interactions. The absence of high-momentum "wings" in the curves of Figs. 8 and 9 indicates that when the two particles are interacting strongly together, they do not often interact strongly with a third particle. As mentioned previously in this article, perhaps the fraction strongly scattered "after" the interaction is a measure of these third-particle interactions.

Since the simple theory of Levinger seems to work well—even quantitatively—we may assume that in nuclear matter the neutron-proton forces are not strongly modified from what they are in deuterium.

Peterson and Roos[7] have recently reported an experiment in which they interpret the production of photostars in heavy elements at high energies to the photoproduction of a meson which is subsequently reabsorbed in the same nucleus. If the results of our experiment are taken, rather than the M.I.T. results uncorrected for scattering or binding energy, then the magnitude of the cross section to be attributed to absorption of photons by neutron-proton pairs is increased substantially, becoming about half of their observed star cross section. Indeed, in heavy elements the nuclear density is somewhat greater, and the volume-to-surface ratio considerably greater than in helium, so that an even greater fraction of their stars may be from this source.

Since mesons are known to be absorbed principally by

[15] J. M. Wilcox and B. J. Moyer, Phys. Rev. **99**, 880 (1955).

[16] R. Hofstadter and G. R. Burlesen, Bull. Am. Phys. Soc. Ser. II, **2**, 390 (1957).

nucleon pairs and since the mean free path of a meson at their energies was found to be less than a meson Compton wavelength, it is not at all clear that meson production and reabsorption is not just another way of describing a photon-nucleon pair interaction. If the complete process is described by $\gamma+2$ nucleons $\rightarrow 2$ nucleons, then there should be selection rules operating which will strongly favor the two nucleons being a neutron and a proton. If the process is described by a mean-free-path argument as $\gamma+$ nucleon $\rightarrow\pi+$ nucleon, $\pi+2$ nucleons $\rightarrow 2$ nucleons, then the two processes would be independent; a π^+ meson could be produced and subsequently reabsorbed by a proton-neutron pair, giving rise, finally, to a pair of correlated fast protons. Proton-proton pairs from the photodisintegration of complex nuclei have been looked for and found only in very small numbers.[17]

ACKNOWLEDGMENTS

The authors would like to thank Dr. Van Nicolai for his operation of the liquid gas target and Mr. R. Harber and Mr. R. C. Herndon for their assistance in various phases of the experimental work. Helpful discussions with G. Ascoli, G. Bernardini, G. F. Chew, and D. G. Ravenhall are also gratefully acknowledged. Thanks are also due A. Wattenberg and V. Z. Peterson for information on their work prior to publication.

[17] Weinstein, Odian, Stein, and Wattenberg, Phys. Rev. **99**, 1620 (1955). J. R. Palfrey, Photonuclear Conference, Case Institute of Technology, Cleveland, Ohio, May, 1955 (unpublished).

PHYSICAL REVIEW VOLUME 110, NUMBER 5 JUNE 1, 1958

Form Factor of the Photopion Matrix Element at Resonance*

W. K. H. PANOFSKY AND E. A. ALLTON
High-Energy Physics Laboratory, Stanford University, Stanford, California
(Received February 6, 1958)

The inelastic scattering of electrons in hydrogen leading to pion formation has been examined. Measurements were carried out in which a hydrogen target was bombarded by electrons of energy E_1 w' h secondary electrons of energy E_2 being detected by a magnetic analyzer at a fixed angle of 75°. The enc ies E_1 and E_2 were programed together such that the pions were produced at a constant energy near the peak of the pion-nucleon resonance in the $(\frac{3}{2},\frac{3}{2})$ state; at the same time the momentum transfer to the pion-nucleon system was varied. Special procedures were developed to eliminate contributions from competing processes. Approximately three fourths of the observed cross section corresponds to magnetic-dipole absorption of the incident virtual photon; the momentum transfer dependence can be interpreted in terms of a form factor of the difference between the magnetic moments of the neutron and proton. If the electron-scattering radii are assumed for the proton, then the data appear to require an rms radius of the magnetic moment of the neutron of about 1.1×10^{-13} cm, based on an exponential model; nucleon recoil corrections are still somewhat uncertain.

I. INTRODUCTION

A. General

IN a series of earlier papers[1–3] we have described our study of the direct production of π mesons in inelastic electron-proton collisions. In the previous experiments the π^+-meson yield from the reaction

$$e+p\rightarrow n+\pi^++e' \qquad (1)$$

was measured and compared with the yield from the photopion process

$$\gamma+p\rightarrow n+\pi^+; \qquad (2)$$

i.e., the yields of π^+ mesons from protons bombarded by real and virtual photons have been compared. The inelastic scattering reaction (1) and the photoproduction process (2) are nearly equivalent with the following basic difference: the interaction Hamiltonian of (2) is the product of the purely transverse photon vector potential with the current operator of the meson-nucleon current, while the corresponding Hamiltonian of (1) is the product of the Møller potential corresponding to the initial and final electron states times the meson-nucleon current. This general fact has the following consequences: (a) In the photoprocess the energy transfer to the nucleon-meson system is equal to the momentum transfer; in the electron process the energy transfer and the momentum transfer can be independently controlled by proper choice of the electron-scattering kinematics. (b) Longitudinal matrix elements can contribute to (1) but not to (2).

In our previous experiments[1–3] the quantitative significance of these effects was very difficult to establish. The reason for this problem is that the Møller potential favors electron-scattering processes where the final electron is directed in the forward direction; for

* Supported in part by the joint program of the Office of Naval Research, the U. S. Atomic Energy Commission, and the U. S. Air Force, Office of Scientific Research.
[1] Panofsky, Newton, and Yodh, Phys. Rev. **98**, 751 (1955).
[2] Panofsky, Woodward, and Yodh, Phys. Rev. **102**, 1392 (1956).
[3] G. B. Yodh and W. K. H. Panofsky, Phys. Rev. **105**, 731 (1957).